Available online at www.sciencedirect.com
SCIENCE DIRECT®
Applied Radiation and Isotopes 61 (2004) 1431–1435
Applied Radiation and Isotopes
www.elsevier.com/locate/apradiso

Theoretical basis for long-term measurements of equilibrium factors using LR 115 detectors

D. Nikezic[1], F.M.F. Ng, K.N. Yu*

Department of Physics and Materials Science, City University of Hong Kong, Tat Chee Avenue, Kowloon Tong, Kowloon, Hong Kong

Received 9 January 2004; received in revised form 18 April 2004; accepted 4 May 2004

Abstract

In this paper, we propose a method to determine the equilibrium factor using a bare LR 115 detector. The partial sensitivities ρ_i of the LR 115 detector to ^{222}Rn and its alpha-emitting short-lived progeny, ^{218}Po and ^{214}Po, were investigated. We first determined the distributions of lengths of major and minor axes of the perforated alpha tracks in the LR 115 detector produced by ^{222}Rn, ^{218}Po and ^{214}Po through Monte Carlo simulations. The track parameters were calculated using a track development model with a published V function, by assuming a removed active layer of 6.54 μm. The distributions determined for different alpha emitters were found to completely overlap with one another. This implied equality of partial sensitivities for radon and its progeny, which was also confirmed through analytical considerations. Equality of partial sensitivities makes possible convenient measurements of the proxy equilibrium factor F_p, which is defined in the present work as $(F_1 + F_3)$ and is equal to the ratio between the sum of concentrations of the two alpha emitting radon progeny (^{218}Po + ^{214}Po) to the concentration of radon gas (^{222}Rn). In particular, we have found $F_p = (\rho/\rho_i t C_0) - 1$, where ρ (track/m^2) is the total track density on the detector, $\rho_i = 0.288 \times 10^{-2}$ m, t is the exposure time and C_0 (Bq/m^3) is the concentration of ^{222}Rn. If C_0 is known (e.g. from a separate measurement), we can obtain F_p. The proxy equilibrium factor F_p is also found to be well correlated with the equilibrium factor between radon gas and its progeny through the Jacobi room model. This leads to a novel method for long-term determination of the equilibrium factor.

Keywords: Natural radioactivity; Radon; Equilibrium factor; LR 115 detector

1. Introduction

Methods for long-term monitoring of the ^{222}Rn gas itself are well established. These include the use of solid-state nuclear track detectors (SSNTDs) (see e.g. Nikolaev and Ilic (1999) for a survey). However, methods for long-term monitoring of the concentrations of radon progeny, or the equilibrium factor (which surrogates the ratios of concentrations of radon progeny to the concentration of the ^{222}Rn gas), are still being explored.

In this paper, we propose to use the bare LR 115 detector (12 μm red cellulose nitrate on a 100 μm clear polyester base, from DOSIRAD, Type 2, Non-Strippable), which is a commonly used SSNTD, for determining the equilibrium factor.

2. Determination of response of LR 115

The first task is to study the partial sensitivities ρ_i of the detector (i.e. the detector sensitivities to radon and

*Corresponding author. Tel.: +852-2788-7812; fax: +852-2788-7830.
E-mail address: peter.yu@cityu.edu.hk (K.N. Yu).
[1] On leave from Faculty of Sciences, University of Kragujevac, Serbia and Monte Negro.

0969-8043/$ - see front matter © 2004 Elsevier Ltd. All rights reserved.
doi:10.1016/j.apradiso.2004.05.065

its progeny). We first determine the distributions of lengths of major and minor axes of alpha tracks in the LR 115 detector produced by ^{222}Rn, ^{218}Po and ^{214}Po. The Monte Carlo program developed earlier by us (Nikezic and Yu, 1999) is employed. However, the concept of effective volume is not used.

A cross section of the sampling volume is shown in Fig. 1. The initial points of alpha particles in the simulations have been chosen in such a way that their distances to the detector are less than the range R of the alpha particles in air. They are also chosen so that the incident angle to the detector is larger than the theoretical critical angle θ_{lim}, which is defined as $\theta_{lim} = \mathrm{a}\sin(1/V_{max})$ where V_{max} is the maximal value of the V function (the ratio of the track etch rate V_t to the bulk etch rate V_b, i.e., $V = V_t/V_b$). Particles striking the detector with an angle smaller than θ_{lim} cannot produce any track.

To determine the incident energy of an alpha particle when it strikes the detector, we employed the SRIM2000 program (Ziegler, 2001). The stopping-power data were used to produce energy–distance tables for alpha particles in air; these are graphically presented in Fig. 2. The energy E_x of the alpha particle incident on the detector after traveling a distance in air was determined by linear interpolation between data in the corresponding energy–distance table. The ranges of alpha particles in the LR 115 detector (cellulose nitrate) were also determined using the data obtained from SRIM2000.

The lengths of major and minor axes were calculated by a model, recently developed by the present authors (Nikezic and Yu, 2003). Additional information, such as the track etch rate V_t and bulk etch rate V_b, were needed to simulate track growth and to calculate the track parameters. The bulk etch rate of the LR 115 detector was indirectly determined by many authors (Somogyi et al., 1978; Nakahara et al., 1980; Sanzelle et al., 1986) through measurements of track radii after irradiation to fission fragments. Direct measurements of V_b were made more recently (Nikezic and Janicijevic, 2002; Yip et al., 2003a, b). In this work, we adopted $V_b = 3.27\,\mu\mathrm{m\,h^{-1}}$, which corresponded to the standard etching conditions:

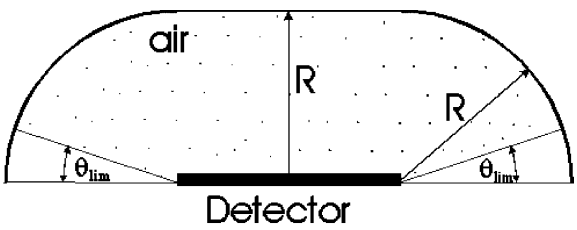

Fig. 1. Cross section of the sampling volume of initial points of alpha particles in the simulation. R is the range of alpha particles in air, while $\theta_{lim} = \mathrm{a}\sin(1/V_{max})$ is the critical angle. The 3D object is obtained by rotation of the curve around the normal onto the detector.

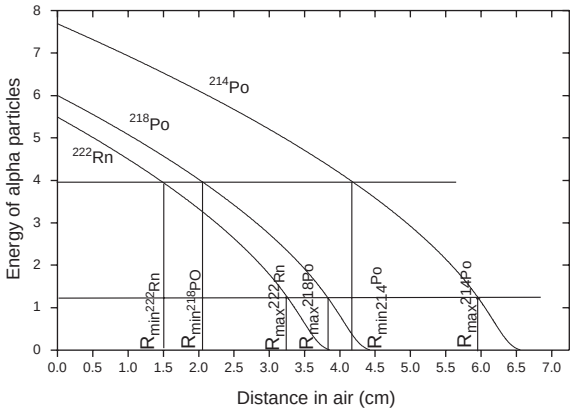

Fig. 2. Energy–distance curves for radon and its progeny in air. The alpha particles emitted from a distance between R_{min} and R_{max} will strike the detector with an energy within the energy window for LR 115 between 1.25 and 3.9 MeV.In all cases, $R_{max} - R_{min} \approx 1.7$ cm (see Table 1).

2.5 N aqueous solution of NaOH at 60°C without stirring (Nikezic and Janicijevic, 2002). Stirring was found to significantly enhance the bulk etch rate to $V_b \approx 7\,\mu\mathrm{m\,h^{-1}}$ (Yip et al., 2003a). Calculations were performed for a removed active layer of 6.54 μm, assuming that the etching lasted for 2 h, which is a common practice for this detector. The initial thickness of LR 115 was taken as 12 μm, as declared by the manufacturer, so the residual thickness of the active layer was 5.46 μm.

Regarding the track etch rate V_t, we adopted the V function ($V = V_t/V_b$), published by Durrani and Green (1984) as

$$V = 1 + (100\mathrm{e}^{-0.446R'} + 5\mathrm{e}^{-0.107R'})(1 - \mathrm{e}^{-R'}). \quad (1)$$

In order to optimize the calculations and to reduce the computational time, prior to the simulations, we produced tables containing data $D_{major}(E,\theta)$ on the major axis and data $D_{minor}(E,\theta)$ on the minor axis by systematically changing the incident energy from 0.1 up to 7 MeV with steps of 0.1 MeV, and incident angle from 20° up to 90° with steps of 1°. Only the tracks which perforate the active layer of the LR 115 detector are considered.

In the simulations, the track parameters were calculated by linear interpolation between the two nearest data points in the tables. In this way, the computation time was significantly reduced, which enabled execution of a large number of simulations, which was 10^6 in our case. As a result, the distributions of track parameters were calculated with small fluctuations.

In the course of simulations, all the tracks were selected according to the lengths of their major and minor axes, with steps of 0.2 μm. When the calculations

were completed, the number distribution N_i was obtained: this is the number of tracks with the length of the major axis between D_i and $D_i + 0.2\,\mu m$. The number distribution is then divided with the total number of the tracks to give the probability distribution p_i, which represents the probability of a particle creating a track with the major axis length between D_i and $D_i + 0.2\,\mu m$. The ratio $p_i/0.2$ is the probability density function f_i (in m^{-1}).

The next step was the multiplication of f_i and $VC\varepsilon t$, where V is the volume (m^3) of the space where the initial points of alpha particles were chosen (Fig. 1), C (Bq/m^3) is the concentration of alpha emitters (radon or radon progeny in our case) in air, ε is the detection efficiency expressed as the ratio between the number of particles creating tracks in the detector to the total number of emitted particles, and t (s) is the time of irradiation. Since VCt is the number of alpha particles emitted in the time interval t in the space above the detector, $VC\varepsilon t$ is the number of the tracks created in the detector. Therefore, the product $f_i VC\varepsilon t$ is the probability density for the given exposure Ct, i.e., the probability to obtain a track with the major axis in the range $(D, D + dD)$ for the exposure Ct. If we assume that $Ct = 1\,Bq\,s\,m^{-3}$, the probability density per unit exposure is obtained. The same formulations will apply for the cases of the minor axis.

3. Results and discussion

3.1. Equality of partial sensitivities

It is interesting to find out that the distribution of the major and minor axes of perforated tracks in the LR 115 detector for three alpha energies in the radon chain overlap completely. The conclusion is that the distributions are independent of the initial energy of the alpha particles. In other words, the partial sensitivities ρ_i of the LR 115 detector to ^{222}Rn, ^{218}Po and ^{214}Po are the same.

The equality among the partial sensitivities is an interesting result. Similar results have been obtained by the previous research but the phenomenon has not been studied in details and has not been explained. For example, Somogyi et al. (1984) found that partial sensitivities in diffusion chambers were equal among themselves if the radius of chamber was larger than 4 cm, and if the progeny was not deposited onto the chamber wall. Under such conditions, the detector operated just like a bare one. The value given by Somogyi et al. (1984) for partial sensitivity was about 0.28×10^{-2} m (as recalculated by the present authors using data from the graph in the original work). Nikezic and Baixeras (1996) calculated partial sensitivities of a bare detector as a function of the removed layer and found that they were very close to each other for the same thickness of removed layer. At that time, they applied the track growth model of Somogyi and Szalay (1973) and got the value $\rho_i = 0.244 \times 10^{-2}$ m for 6 μm of removed layer and $\rho_i = 0.334 \times 10^{-2}$ for 7 μm of removed layer. Linear interpolation gives $\rho_i \approx 0.29 \times 10^{-2}$ m, which is close to the value of 0.288×10^{-2} m obtained here with our model of the track growth. Different models of track growth brought close results for partial sensitivities.

Equality of partial sensitivities means εV is constant, i.e. the product does not depend on the initial alpha particle energy. Let us now calculate the probability dP that an alpha particle emitted at the point $A(r, \theta, \phi)$ hit the point-like detector at the origin of the coordinate system with a surface area dS (see Fig. 3, left panel). The relevant alpha particles are emitted within the hemisphere with radius R, which is the range of these particles in air. The probability dP is given as

$$dP = \frac{dS \cos\theta}{4\pi r^2}. \tag{2}$$

Then the probability per unit surface area of the detector is given as

$$\frac{dP}{dS} = \frac{\cos\theta}{4\pi r^2}. \tag{3}$$

If one considers all the relevant alpha particles in the hemisphere, the average detection efficiency $\bar{\varepsilon}$ per unit detector surface becomes

$$\bar{\varepsilon} = \frac{\int (dP/dS)\, dV}{\int dV} = \frac{\int_0^R \int_0^{2\pi} \int_0^{\pi/2} \frac{\cos\theta}{4\pi r^2} r^2 \sin\theta\, dr\, d\theta\, d\varphi}{\frac{4}{3}(\pi R^3/2)} \tag{4}$$

or simply

$$\bar{\varepsilon} = \frac{3}{8\pi R^2}. \tag{5}$$

If the radionuclide concentration in air is C (Bq/m^3), a total of VC of alpha particles will be emitted in 1 s within the hemispherical volume. The number of hits

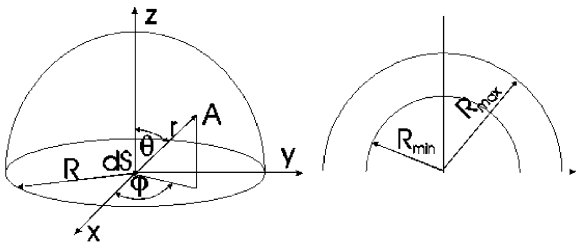

Fig. 3. Left panel: Geometry of the irradiation volume for explanation of equality of the partial sensitivities. Right panel: cross section of the reduced integration volume, with R_{min} and R_{max} corresponding to the energy detection limits.

per second, N, will be

$$N = \bar{\varepsilon} VC = \frac{3}{8\pi R^2}\frac{4}{3}\frac{\pi R^3}{2}C = \frac{1}{4}RC \quad (6)$$

which is known as Cherry's formula (Cherry, 1964).

Eq. (5) shows that the average detection efficiency is inversely proportional to the surface area of the hemispherical volume. However, as mentioned above, the equality of partial sensitivities found from our Monte Carlo simulations implies a constant εV, so the efficiency should be inversely proportional to the effective volume. The discrepancy is caused by the upper and lower energy detection limits of the LR 115 detector. The above derivation should be modified to take these into account. Instead of performing the integration in Eq. (4) from 0 to R, it should be performed from R_{min} up to R_{max}, which correspond to the energy detection limits. If an alpha particle is emitted beyond R_{max}, it will be slowed down too much in the air and hit the detector with an energy lower than E_{min}. On the other hand, if it is emitted at a distance smaller than R_{min}, it cannot be sufficiently slowed down to hit the detector with an energy smaller than the upper energy limit E_{max}. In other words, only particles emitted between R_{min} and R_{max} can generate perforated tracks in the LR 115 detector. In Fig. 3 (right panel), the cross section of the trimmed integration volume is shown. All integrations in Eq. (4) remain the same except that the integration with respect to the variable r is from R_{min} to R_{max}, i.e.

$$\int_{R_{min}}^{R_{max}} \mathrm{d}r = (R_{max} - R_{min}) \quad (7)$$

so the final expression for the average detection efficiency becomes

$$\bar{\varepsilon} = \frac{3}{8\pi R^3}(R_{max} - R_{min}). \quad (8)$$

To calculate R_{min} and R_{max} for energies of alpha particles in the radon chain, we used data for stopping power for alpha particles in air given by the SRIM2000 program and the energy–distance tables mentioned above. On determining from our calculations the upper and lower energy limits for the LR 115 detector to be 3.9 and 1.25 MeV, respectively, we calculated the values of R_{min} and R_{max} as shown in Table 1. These values are also shown in Fig. 2. In the calculations, we only considered the tracks with both major and minor axes longer than 1 μm. As the difference $(R_{max} - R_{min}) \approx 1.7$ cm = constant, the efficiency is inversely proportional to R^3, i.e. $\varepsilon V \approx$ constant.

This is a simplified explanation for the equality of the partial sensitivities. Here, a point-like detector was considered and the critical angle has not been considered, but the results are qualitatively the same in the realistic case.

Table 1
The values of R_{min} and R_{max} calculated for energies of alpha particles in the radon chain using data for stopping power given by the SRIM2000 program

Alpha energy (MeV)	Range (cm)	R_{min} (cm)	R_{max} (cm)	$R_{max} - R_{min}$ (cm)
5.49	3.85	1.5	3.25	1.75
6.00	4.42	2.1	3.82	1.72
7.69	6.55	4.2	5.95	1.75

3.2. Equilibrium factor determination

Since the distribution of the major and minor axes of perforated tracks in the LR 115 detector for different alpha emitters overlap, the partial sensitivities ρ_i are equal to one other. By integration of the corresponding curves, we found that the partial sensitivities ρ_i are

$$\rho_i = \rho_{^{222}\mathrm{Rn}} = \rho_{^{218}\mathrm{Po}} = \rho_{^{214}\mathrm{Po}} = 0.288 \times 10^{-2}\ \mathrm{m}. \quad (9)$$

Therefore, the total sensitivity in the case of radioactive equilibrium between radon and its progeny will be $\rho_{^{222}\mathrm{Rn}} + \rho_{^{218}\mathrm{Po}} + \rho_{^{214}\mathrm{Po}} = 0.864 \times 10^{-2}$ m. In case of disequilibrium, the total track density ρ (in track/m^2) on the detector is

$$\rho = \rho_i(C_0 + C_1 + C_3) \cdot t, \quad (10)$$

where C_0, C_1 and C_3 are concentrations of ^{222}Rn, ^{218}Po and ^{214}Bi(Po) in Bq/m^3 and t is the exposure time. If the radon concentration C_0 is known (e.g. from a separate measurement), we can obtain the sum $(C_1 + C_3)$ given as

$$C_1 + C_3 = \frac{\rho}{\rho_i t} - C_0. \quad (11)$$

If one divides by C_0, this becomes

$$F_p = F_1 + F_3 = \frac{C_1}{C_0} + \frac{C_3}{C_0} = \frac{\rho}{\rho_i t C_0} - 1, \quad (12)$$

where F_p is a sum of F_1 and F_3, and is given the name "proxy equilibrium factor".

A similar quantity, called the reduced equilibrium factor F_{red}, introduced recently by Amgarou et al. (2003) was defined as $F_{red} = 0.105F_1 + 0.380F_3$. It has been shown that the equilibrium factor can be determined if F_{red} is known. Amgarou et al. (2003) calculated equilibrium factors through the Jacobi room model (Jacobi, 1972) by systematically varying all parameters that influence the concentrations of radon and its progeny, and plotted them with F_{red}. We repeat the procedures here, but replace F_{red} with F_p; the results are shown in Fig. 4. One may observe that the proxy equilibrium factor has a good correlation with the equilibrium factor F, so we have effectively found a convenient method for the determination of F with the LR 115 detector. The method proposed by Amgarou et al. (2003), through the reduced equilibrium factor

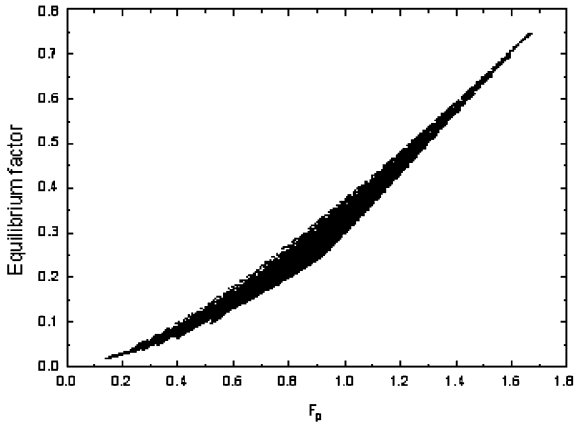

Fig. 4. Dependence of the equilibrium factor F on the proxy equilibrium factor $F_p(= F_1 + F_3)$.

F_{red}, involved measurements of ^{218}Po and ^{214}Po concentrations. These relied on particular etching conditions on the Makrofol detector to enable the counting of alpha tracks in two energy windows, viz., (3–5 MeV) for ^{222}Rn and ^{218}Po, and (6.3−7.5 MeV) for ^{214}Po. The method proposed in the present paper is much simpler and more convenient.

Acknowledgements

The present research is supported by the CERG grant CityU1081/01P from the Research Grant Council of Hong Kong.

References

Amgarou, K., Font, Ll., Baixeras, C., 2003. A novel approach for long-term determination of indoor ^{222}Rn progeny equilibrium factor using nuclear track detector. Nucl. Instrum. Methods A 506, 186–198.

Cherry, R.D., 1964. In: Adams, J.A.S. (Ed.), The Natural Radiation Environment. Univ. of Chicago Press, Chicago, pp. 407–424.

Durrani, S.A., Green, P.F., 1984. The effect of etching conditions on the response of LR 115. Nucl. Tracks 8, 21–24.

Jacobi, W., 1972. Activity and potential α energy of ^{222}Rn and ^{220}Rn daughters in different air atmosphere. Health Phys. 22, 441–450.

Nakahara, N., Kudo, H., Akiba, F., Murakami, Y., 1980. Some basic studies on the absolute determination of radon concentration in the air by a cellulose nitrate detector. Nucl. Instrum. Methods 171, 171–179.

Nikezic, D., Baixeras, C., 1996. Radon, radon progeny and equilibrium factor determination using an LR 115 detector. Radiat. Meas. 26, 204–213.

Nikezic, D., Janicijevic, A., 2002. Bulk etching rate of LR-115 detectors. Appl. Radiat. Isotopes. 57, 275–278.

Nikezic, D., Yu, K.N., 1999. Determination of deposition behaviour of ^{218}Po from track density distribution on SSNTD in diffusion chamber. Nucl. Instrum. Methods A 437, 531–537.

Nikezic, D., Yu, K.N., 2003. Three-dimensional analytical determination of the track parameters: over-etched tracks. Radiat. Meas. 37, 39–45.

Nikolaev, V.A., Ilic, R., 1999. Etched track radiometers in radon measurements: A review. Radiat. Meas. 30, 1–13.

Sanzelle, S., Fain, J., Mialler, D., 1986. Theoretical and experimental study of alpha counting efficiency using Kodak SSNTD applied to dosimetry in the field of thermoluminescence dating. Nucl. Tracks 12, 913–916.

Somogyi, G., Hunyadi, I., Varga, Zs., 1978. Spark counting technique of α-radiograms recorded on LR 115 strippable cellulose nitrate film. Nucl. Track Detect. 2, 191–197.

Somogyi, G., Paripas, S., Varga, Zs., 1984. Measurements of radon, radon daughters and thoron concentrations by multi-detector devices. Nucl. Tracks Radiat. Meas. 8, 423–427.

Somogyi, G., Szalay, S.A., 1973. Track-diameter kinetics in dielectric track detectors. Nucl. Instrum. Methods 109, 211–232.

Yip, C.W.Y., Ho, J.P.Y., Koo, V.S.Y., Nikezic, D., Yu, K.N., 2003a. Effects of stirring on the bulk etch rate of LR 115 detector. Radiat. Meas. 37 (2003), 197–200.

Yip, C.W.Y., Ho, J.P.Y., Nikezic, D., Yu, K.N., 2003b. A fast method to measure the thickness of removed layer from etching of LR-115 detector based on EDXRF. Radiat. Meas. 36, 161–164.

Ziegler, J.F., 2001. SRIM-2000, http://www.srim.org/.